Electric-field tunnel effects in EPR of paraelectric centers

A. B. Roĭtsin, A. B. Brik, and V. L. Gokhman

(Submitted 28 July 1987)
Zh. Eksp. Teor. Fiz. **94**, 194–203 (May 1988)

A theoretical and experimental investigation was carried out of tunneling, between various structural positions in a crystal, by microparticles coupled to centers that have simultaneously paraelectric and paramagnetic properties, in the presence of electric (**E**) and magnetic (**H**) fields. It is established that electric-field effects of a qualitatively novel type are possible in EPR of the systems considered. The experiments were performed by the EPR method on quartz crystals with low-symmetry Al-O$^-$ centers, in which a paramagnetic hole can be localized on one of the two oxygen ions of the AlO_4 tetrahedron, or can become delocalized relative to these ions. An anomalous influence of the electric fields in the EPR signal intensity was observed at $T \approx 30$ K. The dependences of the effect on the orientations of **E** and **H**, as well as on the intensity of the field **E**, and on the number of defects in the crystals, are investigated.

1. INTRODUCTION

Investigation of tunneling by microparticles is essential for the solution of many problems in physics, chemistry, biology, and engineering.[1-4] Detailed information on tunneling in a solid is obtainable by microwave-spectroscopy methods, such as paraelectric resonance[5-7] which is observed in centers having electric dipole moments and tunneling through the crystal. If the tunneling paraelectric centers are furthermore paramagnetic, observation of EPR on them in the presence of external electric fields provides unprecedented opportunities of obtaining information on microparticle tunneling.

Various electric-field effects in EPR of localized centers have by now been thoroughly investigated.[6,8] Relaxation of tunneling centers was considered in Refs. 10–13, and the influence of an electric field on a system with a threefold degenerate electron ground term of symmetry T_d was investigated in Ref. 14. It can nevertheless be stated that there are no published reports on the influence of electric fields on the frequencies and probabilities of EPR transitions of delocalized paraelectric centers. To a considerable degree, this is due to the fact that until recently a theory of electric-field effects in EPR was developed only for paramagnetic impurity centers with fixed positions in the crystal. At the same time, paramagnetic paraelectric centers that tunnel through crystals are quite frequently encountered. Foremost among them are orientation-changing electron-hole centers. These objects, as will be shown below, are subject to qualitatively new electric-field effects of a type that differs from the traditional ones.[6,8,9]

Tunneling studies by microwave-spectroscopy methods were confined as a rule to high-symmetry cubic centers. Recently, however, active research into low-symmetry centers using microwave spectroscopy have been initiated.[15] It is important therefore to increase the number of objects in which tunneling effects due to low-symmetry system can be occur. A distinctive feature of these systems is the presence of an adiabatic potential with a small number of wells, so that they can be treated as appropriate model systems. At the same time, the large number of parameters of the external actions can lead to a large number of effects related both to the orientation of the fields and to their absolute values.

2. THEORY

1. Following Ref. 7, we assume the following: 1) Local symmetry of the paramagnetic center (PC) in the initial symmetric nonequilibrium position corresponds to the point group C_{2v}. 2) Tunneling between two equivalent minima of the adiabatic potential leads to a two-level system with tunnel splitting Δ, i.e., the vibron problem has been solved. In addition to the assumptions of Ref. 7, we recognize here that each of the levels is doubly degenerate in spin. We characterize the lower and upper levels by irreducible representations (IR) Γ_5 and $\Gamma_5^{(1)}$ respectively (see Ref. 16 for the designations of the IR). The z axis of the rectangular coordinate system is chosen along a twofold axis, and the x and y axes in reflection planes. We assume that the minima of the adiabatic potential (the wells) lie on the y axis. The influence of the electric and magnetic fields is described by the matrix M_s of the perturbation operator—$\mu\cdot\mathbf{H}-\mathbf{d}\cdot\mathbf{E}$, where μ and d are the effective magnetic and electric dipole moment of the PC. Numbering the wave functions in the sequence $\psi_1^{\Gamma_5}, \psi_2^{\Gamma_5}, \psi_1^{\Gamma_5(1)}, \psi_2^{\Gamma_5(1)}$, we obtain[16] for the matrix elements (ME) of the matrix M_s, whic includes also the gap Δ,

$$\begin{gathered} M_{11,\,22}=\alpha E_z-\Delta/2\pm\beta_1 H_z, \quad M_{33,\,44}=\alpha_1 E_z+\Delta/2\pm\beta_4 H_z, \\ M_{12,\,34}=\beta_{2,\,5}H_x+i\beta_{3,\,6}H_y, \quad M_{13,\,24}=i(\alpha_2 E_z\pm\beta_7 H_z), \\ M_{14,\,23}=\alpha_4 E_y\pm\beta_9 H_y+i(\beta_8 H_x\pm\alpha_3 E_x), \quad M_{kl}=M_{lk}^*. \end{gathered} \tag{1}$$

The constants α and β are the ME of the operators $-d_i$ and μ_i, respectively. For example,

$$i\alpha_3=\int \psi_1^{\Gamma_5}(-d_x)\,\psi_2^{\Gamma_5^{(1)}}\,d\tau.$$

We refer to the representation that leads to the matrix M_s as symmetrized.

We transform from the symmetrized representation (1) to a well representation by using the unitary transformation

$$M_w=S^{-1}M_cS, \tag{2}$$

where the nonzero matrix elements of S are $S_{11}=S_{13}=S_{22}=S_{24}=S_{32}=-S_{34}=S_{41}=-S_{43}=1/2$. The ME of the matrix M_w contain, besides the parameters of M_s, also the linear combinations

 0038-5646/88/050975-06$04.00

$$\beta_{ij}^{\pm}=(\beta_i\pm\beta_j)/2,\quad \alpha_{01}^{\pm}=(\alpha\pm\alpha_1)/2,\quad \Delta^*=\alpha_{01}^{-}E_z-\Delta/2. \quad (3)$$

The row and column numbering that follows from (2) for the matrix M_w corresponds to the sequence $\varphi_1^-, \varphi_1^+, \varphi_2^-, \varphi_2^+$ (φ_i^ρ is a function of the ith well with spin projection ρ). Note that it is convenient to use the matrix M_w in the case of weak tunneling and the matrix M_s for strong tunneling.

2. Since our aim is an approximate solution of the problem, we perform beforehand one more unitary transformation of the matrix M (M_s or M_w):

$$\overline{M}=U^{-1}MU, \quad (4)$$

in a representation in which the 2×2 blocks along the principal diagonal ar diagonalized ($\overline{M}_{12}=\overline{M}_{34}=O$), and U is a quasi-diagonal matrix. Without writing out the general expressions for U_{ij} and $\overline{M}_{ij}$ (in the form of ME of the matrix M), we write, only as an example which we shall use below, the diagonal ME of the matrix M_w already in explicit form

$$\overline{M}_{11,\,22}=l_0+\alpha_4E_y\pm r^+,\quad \overline{M}_{33,\,44}=l_0-\alpha_4E_y\pm r^-, \quad (5)$$

where

$$r^{\pm}=\Big[\sum_s (g_sH_s)^2\pm 2g_{zy}'H_zH_y\Big]^{1/2},$$

$$g_x^2=(\beta_{25}^+)^2,\quad g_y^2=\beta_9^2+(\beta_{36}^-)^2, \quad (6)$$

$$g_z^2=\beta_7^2+(\beta_{14}^-)^2,\quad g_{zy}'=\beta_9\beta_{14}^-+\beta_7\beta_{36}^-,\quad l_0=\alpha_{01}^+E_z.$$

The subscript s numbers the axes x, y, and z.

3. Let us find approximate solutions for the matrix M. We choose its diagonal ME as the zeroth approximation, and the remaining ME as a perturbation. This means smallness of the ME of the intertunnel states in the case of M_s and of the ME between the different wells in the case of M_w. Analysis of expressions (5) and (6) shows that cases when $\overline{M}_{11}=\overline{M}_{33}$, $\overline{M}_{22}=\overline{M}_{44}$ or $\overline{M}_{11}=\overline{M}_{44}$, $\overline{M}_{22}=\overline{M}_{33}$, (i.e., degeneracy or close placement of two levels) are possible at definite orientations and values of the fields **E** and **H**. It is convenient therefore to develop the theory for the case in a way that one pair (our of the four) levels is considered exactly, and the ME between the states of different pairs are treated as a perturbation. To make the approach general, the distance between the levels in the pair must be regarded as arbitrary rather than small or zero. This problem is considered in general form in the Appendix.

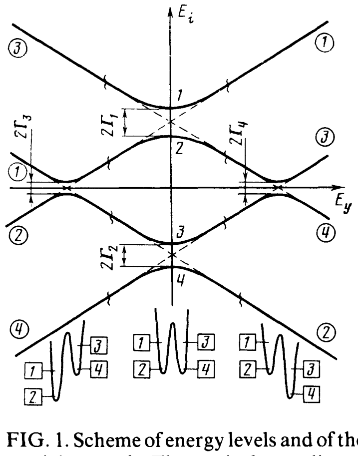

FIG. 1. Scheme of energy levels and of the two-well potentials in which the particle tunnels. The vertical wavy lines separate region I from regions II. The numbers i in the small square correspond to expression (5), and the numbers i in the small circles to expression (8).

4. We present the calculation results for the matrix M_w in the case when the field **H** is directed along an arbitrary coordinate axis s. We note beforehand, however, that it follows from (5) that at different values of E_y one and the same level can cross different levels (Fig. 1, dashed line). We therefore divide the range of variation of E_y ($-\infty$ to $+\infty$) into two regions. We choose the boundaries of the regions arbitrarily at the points $E_y^b=\pm g_sH_s/2\alpha_4$. It is important, however, to have the distance between levels near the boundary large enough for perturbation theory to be applicable. The energy structure is of the form:

1) Region I ($|E_y|\leqslant|E_y^b|$):

$$E_{1,\,2}=l_0+l_5^+\pm(\alpha_4^2E_y^2+|\Gamma_1|^2)^{1/2},$$
$$E_{3,\,4}=l_0+l_5^-\pm(\alpha_4^2E_y^2+|\Gamma_2|^2)^{1/2},$$
$$\Gamma_{1,\,2}=l_1^\pm+il_2^\pm. \quad (7)$$

2) Region II:

$$E_{1,\,2}=l_0\pm[(\alpha_4E_y+l_5^+)^2+|\Gamma_3|^2]^{1/2},$$
$$E_{3,\,4}=l_0\pm[(\alpha_4E_y+l_5^-)^2+|\Gamma_4|^2]^{1/2},$$
$$\Gamma_{3,\,4}=l_3^\pm+il_4^\pm, \quad (8)$$

where

$$(l_1^\pm)_x=\Delta^*\pm\xi_x\beta_{25}^-H_x,$$
$$(l_1^\pm)_y=\xi_y[(\beta_{36}^-\Delta^*-\beta_9\alpha_2E_z)/g_y\pm\beta_{36}^+H_y],$$
$$(l_1^\pm)_z=\beta_{14}^+H_z\pm(\beta_{14}^-\Delta^*+\beta_7\alpha_2E_z)/g_z,\quad (l_2^\pm)_x=\beta_8H_x\pm\xi_x\alpha_2E_z,$$
$$(l_3^\pm)_y=(\beta_9\Delta^*+\beta_{36}^-\alpha_2E_z)/g_y,\quad (l_3^\pm)_z=\xi_z(\beta_7\Delta^*-\beta_{14}^-\alpha_2E_z)/g_z,$$
$$(l_5^\pm)=\pm g_sH_s,\quad \xi_x=\beta_{25}^+/|\beta_{25}^+|,$$
$$\xi_y=\beta_{36}^-/|\beta_{36}^-|,\quad \xi_z=\beta_7/|\beta_7|,$$
$$(l_2^\pm)_z=(l_4^\pm)_x=(l_4^\pm)_y=\alpha_3E_x,\quad (l_2^\pm)_y=(l_3^\pm)_x=(l_4^\pm)_y=0.$$

Terms of second order of smallness [the second term of (A.1)] have been left out of Eqs. (7) and (8), since analysis has shown them to have no effect on the main conclusions of the work. The numbering of the levels in Eqs. (7) and (8) is in accord with the pairwise grouping of the levels in each of the region. Figure 1 (solid line) shows the energy structure in accordance with Eqs. (7) and (8).

We present the expressions obtained for the transition ME from the equations of the Appendix (the numbering is the same as in Eqs. (7) and (8)).

1) $\mathbf{H}\|x$

$$\gamma_{12,34}=\alpha_4E_y(t)Q_{12,\,34}. \quad (9)$$

Other transitions (13, 24, 14, 23):

$$\gamma_{ij}=H_z(t)(\beta_{14}^-Q_{ij}^+-i\beta_7\xi_xQ_{ij}^-)+H_y(t)(\beta_9Q_{ij}^--i\beta_{36}\xi_xQ_{ij}^+). \quad (10)$$

1) $\mathbf{H}\|y(z)$

$$\gamma_{12,\,34}=Q_{12,\,34}[\alpha_4E_y(t)+H_{z(y)}(t)g_{zy}'/g_{y(z)}]. \quad (11)$$

Other transitions:

$$\gamma_{ij}\approx\xi_{y(z)}Q_{ij}^\pm[\pm H_{z(y)}(t)\bar{g}_{zy}/g_{y(z)}+iH_x(t)\beta_{25}^+]. \quad (12)$$

The upper sign in (12) corresponds to $\mathbf{H}\|y$, and the lower to $\mathbf{H}\|z$, $\bar{g}_{zy}=\beta_{36}^-\beta_{14}^- -\beta_7\beta_9$. The expressions for Q_{ij} are too unwieldy to write out here (plots of some of them are shown in Fig. 2). Equations (9)–(12) illustrate clearly the selection rules.

Equations (7) and (8) wer used to obtain expressions for the transition frequencies ν_{ij} and for the resonant mag-

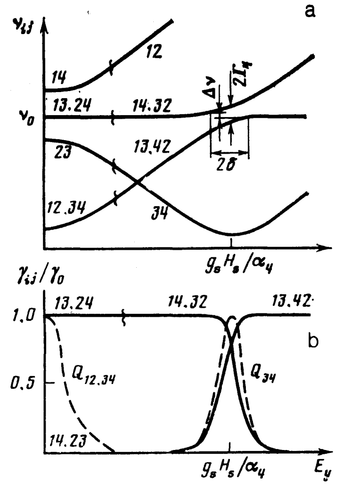

FIG. 2. The resonant frequencies (a) and the ME of the EPR transition probabilities (b) vs the electric field. The subscripts ij label the transitions in accordance with the numbering of the levels in Fig. 1. The dashed lines are plots of $Q_{1,2,3,4}$ that determine the probabilities of the paraelectric transitions vs E_y. $\nu_0 = 2I_5 + /h$, and γ_0 is the value of γ_{ij} in the absence of tunneling. The plots for negative E_y are mirror images of Figs. 1 and 2.

netic-field values H_r. Plot of ν_{ij} and γ_{ij} vs the electric field are shown in Fig. 2. They correspond to a definite (discussed below) relation, typical of centers with weak tunneling, between the parameters of the theory.

3. EXPERIMENT

The measurements were performed with a superheterodyne EPR spectrometer in the 3-cm band. The EPR signals were recorded from an oscilloscope screen with the constant magnetic field modulated by a 50-Hz field. The sample, equipped with coated graphite electrodes, was placed in a teflon ampoule filled with transformer oil.

The principal measurements were made on samples of synthetic pleochroic quartz, with only one of the three Si^{4+} positions predominantly replaced by Al^{3+}. In this isomorphous substitution, one of the oxygen ions of the AlO_2 tetrahedron loses an electron, and Al-O^- centers are produced.[18] We shall designate by O_1 and O_2 the oxygen ions on which paramagnetic holes (spin $S = 1/2$) can be localized. The symmetry of the Al position in the quartz corresponds to the group C_2. If we confine ourselves to the AlO_4 tetrahedron, however, this symmetry can correspond approximately to group C_{2v}. The z axis is then directed along L_2', which is one of the twofold axes of the crystal and which passes through the AlO_4 tetrahedron from which the EPR signal is received, the y axis is directed along the O_1-O_2 direction, and the z axis is perpendicular to the other two directions.

According to Ref. 19, at $T = 4.2$ K a constant electric field alters the intensities of the EPR signals V_1 and V_2 corresponding to hole localization on the O_1 and O_2 ions. This is due to a redistribution of the holes over the positions of these ions. The total EPR signal intensity $V = V_1 + V_2$, however, remains unchanged in this case (if there is no EPR-signal saturation). We have observed that at $T \approx 30$ K the electric field E increases the total intensity of the EPR signals. The experimental results are shown in Figs. 3 and 4. We measured in the experiment the signal peak intensity V corresponding to the center of the EPR line. No noticeable

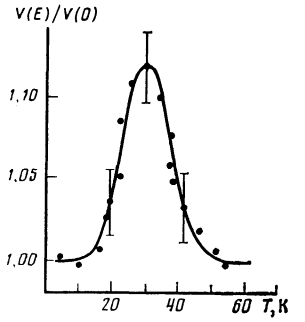

FIG. 3. Temperature dependence of a change produced in the EPR signal by a field $E = 50$ kV/cm, $\widehat{\mathbf{E}L_2'} = 60°$, $\mathbf{E} \perp L_3$, $\mathbf{H} \| L_2'$.

changes of the width and shape of the EPR signals by the field E were recorded. The EPR linewidth at half-maximum was 0.2 Oe. It is difficult to measure accurately the shapes of such narrow EPR lines. The plots shown in Figs. 3 and 4 are independent of the polarity of the electric field and correspond to the case when the EPR signals are not saturated by the microwave field. The $V(E)/V_{max}$ dependence changes with increase of saturation, viz., a large E begins to decrease the EPR signal, apparently because of the effect of E on the spin-lattice relaxation of the Al-O^- centers, an effect described in Ref. 13.

The measurements were made mainly at $\mathbf{H} \| L_2'$ and $\widehat{\mathbf{E}L_2'} = 60°$, $\mathbf{E} \perp L_3$ (is the threefold axis). A study of the dependence of the effects shown in Figs. 3 and 4a on the orientation of the fields $\mathbf{E}$ and $\mathbf{H}$ relative to the crystal axes was made difficult by the smallness of the effects and by superposition of EPR signals from the centers corresponding to Al^{3+} in other sparsely occupied positions of Si^{4+}. At the same time, we succeeded in establishing the following. The effect takes place at $\mathbf{E} \| L_3$ and is absent at $\mathbf{E} \| L_2'$. If the crystal is rotated in a magnetic field around the L_3 axis, the value of $V(E)/V(0)$ changes little, and the effect tends to increase as $\mathbf{H}$ approaches L_2'. Conversely, if the crystal is rotated around the L_2' axis the $V(E)/V(t)$ effect is essentially anisotropic. When the field $\mathbf{H}$ is oriented close to the O_1-O_2 direction, the effect is a maximum is approximately of the same size as at $\mathbf{H} \| L_2'$, while for $\mathbf{H}$ oriented near the x axis (in which case the EPR line is located in the strongest magnetic field), the effects shown in Figs. 3 and 4 are absent.

The foregoing effects were observed, besides in synthetic quartz, also in natural samples of smoky quartz. We did not succeed in observing these effects in samples of honeycomb or morion quartz, which contain more defects.

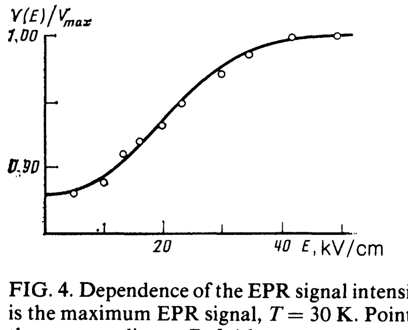

FIG. 4. Dependence of the EPR signal intensity on the electric field, V_{max} is the maximum EPR signal, $T = 30$ K. Points—experiment, solid line—theory according to Ref. 16.

4. COMPARISON OF THEORY AND EXPERIMENT. DISCUSSION OF RESULTS

In real crystals, resonant centers are acted upon, besides the external electric field **E**, also by internal electric fields **e** due to lattice defects, so that the resultant field is $\vec{\mathscr{E}} = \mathbf{E} + \mathbf{e}$. Let $f_i(e_i)$ be the distribution function, normalized to unity, of the ith component of the field **e**. The general expression for the EPR line shape can be represented in the form

$$V(E)=c\iiint_{-\infty}^{+\infty}\prod_{k=1}^{3} f_k(e_k)\sum_j w_j g(\nu-\nu_j)\,de_k, \tag{13}$$

where c is a dimensional factor that includes the density of the centers; $g(\nu - \nu_j)$ is a function of the profile of a line with resonant frequency ν_{ji} (we denote its halfwidth by $\delta\nu_j$); w_j is the square modulus of the ME transition. The summation in (13) is over all possible transitions. If, however, the investigation is carried out at frequencies close to a definite resonant frequency ν_l, the contribution from transitions with $l' \neq l$ can be neglected, inasmuch as $|\nu - \nu_{l'}| \gg \delta\nu_{l'}$ for these transitions and $g(\nu - \nu_l') \approx 0$ can be neglected. In accordance with the experimental conditions we confine ourselves to EPR transitions at the frequency ν_0 (Fig. 2a). Since the components E_x and E_z enter in the theory in the form of perturbation-theory corrections and experiment has revealed no influence of such fields on the frequencies and intensities of the transitions, we neglect herafter these influences ($\alpha_2 = \alpha_3 = 0$, $\alpha_{01} - E_z \ll \Delta/2$), so that only integration with respect to de_y remains in (13).

The dependence of ν_l on w_l on the electric fields is determined by the ratio of the parameters of the theory. Analysis shows that for $|\beta_s H_s| \gg |\Delta|$, where $\beta_x = \beta_{25}^-$, $\beta_y = \beta_{36}^+$, $\beta_z = \beta_{14}^+$, the frequencies and probabilities of the EPR transitions in region I can depend substantially on the field E. The parameter β_s can be interpreted as the magnetic moment induced along the s axis by the tunneling of the charge. The presence of the magnetic moment β_s can lead to various effects on strongly tunneling centers, for example to the onset of magnetic ordering of the centers as the crystal is cooled. If, however, $|\beta_s H_s| \ll \Delta$ we obtain in region I $\omega_{14} = \omega_{23} = 0$, $\omega_{13} = \omega_{24} = \omega_0$, and $\nu_{13} = \nu_{24} = \nu_0$, so that the EPR does not depend on the electric field and coincides with the signal from the localized centers. Analysis shows that the parameters β_s and β_8 for weakly tunneling centers, such as the Al-O^- centers, are negligibly small.

In region II there is produced near the level "crossing" a field interval δE in which the frequencies and probabilities of all the transitions are unequal to the corresponding values for localized centers. This can lead to a dependence of the EPR signal intensity on the field E. We represent expression (13) in the form

$$V(E) = V_{max} - \delta V(E), \tag{14}$$

where $\delta V(E)$ contains integration over the region in which the inequality noted above takes place, and $V_{\max} = cw_0 g(0)$. For $\delta\nu \gg |\Gamma_{3,4}|$ we have $\delta V(E) = 0$, and in the opposite case

$$\delta V(E) = 2V_{max}\delta E[f(E_0-E_y)+f(E_0+E_y)], \tag{15}$$

where $E_0 = g_s H_s/\alpha_4$ and $\delta E \approx 0{,}5|\Gamma_{3,4}|^2\alpha_4^{-1}\delta\nu$ is a deviation of $\mathscr{E}_y$ from E_0 such that $g(\nu_0 - \nu_j) = 0{,}5g(0)$. Expressions (14) and (15) can be interpreted as follows: The delocalized centers for which $\mathscr{E}_y$ lies in the interval $|E_0 \pm \delta E|$ make no contribution to the EPR signal at the frequency ν_0. When an external field that "shifts" the distribution function is applied to the sample, the number of these centers decreases, making the EPR signal stronger. We choose $f_k(e_k)$ to be a Gaussian with half-width $\tilde{E}$ (Ref. 7) and obtain then for $V(E)$

$$\frac{V(E)}{V_{max}} = 1 - \frac{2\delta E}{\pi^{1/2}\tilde{E}}\left\{\exp\left[-\left(\frac{E_0-E_y}{\tilde{E}}\right)^2\right] + \exp\left[-\left(\frac{E_0+E_y}{\tilde{E}}\right)^2\right]\right\}. \tag{16}$$

The value of $\tilde{E}$ for quartz crystals was the subject of a number of studies (e.g., Refs. 7 and 13), according to which $\alpha_4\tilde{E} \approx (10^{10} - 10^{12})$ Hz (we put $h = 1$). The values of E_0 and $\delta\nu$ are known directly from experiment: $\alpha_4 E_0 = g_s H_s = \nu_0/2 = 0{,}5\cdot 10^{10}$ Hz and $\delta\nu = 3\cdot 10^5$ Hz. For $\alpha_4\tilde{E} = 3\cdot 10^{10}$ Hz (which is close to the value of $\alpha_4\tilde{E}$ determined for the investigated sample by independent methods[7,13] and for $\Gamma_{3,4} = 3\cdot 10^7$ Hz the relation (16) agrees with experiment satisfactorily (Fig. 4). With increasing defect content in the crystals, $\alpha_4\tilde{E}$ increases and then, according to (16), the effect of the electric fields on the EPR signal weakens, and this explains the absence of effects in samples with large defect contents.

The influence of the E-field on the EPR signal is approximately the same at $\mathbf{H}\|z$ and $\mathbf{H}\|y$ and is nonexistent at $\mathbf{H}\|x$. In accordance with the foregoing this means that $|\Gamma_{3,4}|$ has for $\mathbf{H}\|z$ and $\mathbf{H}\|y$ approximately equal values $|\Gamma_{3,4}| \gg \delta\nu$, whereas for $\mathbf{H}\|x$, on the contrary, $|\Gamma_{3,4}| \ll \delta\nu$. An explanation of this angular dependence of the effect follows from Eqs. (7) and (8), according to which

$$|\Gamma_{3,4}^x| = 0, \quad |\Gamma_{3,4}^y| \approx \Delta^*\beta_9/g_y, \quad |\Gamma_{3,4}^z| \approx \Delta^*\beta_7/g_z.$$

To estimate these quantities, we compare the parameters contained in Eq. (5) (this equation corresponds to isolated wells) with the parameters of the spin-Hamiltonian of a spin-1/2 particle:

$$2g_z = \beta_0(g_{zz}^2 + g_{zy}^2)^{1/2}, \quad 2g_y = \beta_0(g_{yy}^2 + g_{zy}^2)^{1/2}, \quad 2\beta_7 = 2\beta_9 = \beta_0 g_{zy}, \tag{17}$$

where β_0 is the Bohr magneton and g_{ij} are the components of the g-tensor of the particle. Taking into account the numerical values of the g-tensor of the Al-O^- centers in quartz,[18] we obtain from (17) $|\Gamma_{3,4}^y| = 1{,}14\cdot\Delta^*\cdot 10^{-2}$, $|\Gamma_{3,4}^z| = \Delta^*\cdot 1{,}17\cdot 10^{-2}$. Since experiment yields $|\Gamma_{3,4}| = 3\cdot 10^7$ Hz, we obtain for $T = 30$ K $\Delta^* = 3\cdot 10^9$ Hz. For $T = 4.2$ K we have for th investigated object, according to Ref. 7, $\Delta^* \approx 10^6$ Hz. For $T = 4.2$ we have accordingly $|\Gamma_{3,4}^z| = |\Gamma_{3,4}^y| = 10^4$ Hz $\ll \delta\nu = 3\cdot 10^5$ Hz., so that the theory explains also the fact that the field E does not influence the total signal of the Al-O^- centers in quartz at $T = 4.2$ K.

The causes of the increase of Δ^* of the investigated object at $T \approx 30$ K compared with Δ^* at $T = 4.2$ K are not known at present. We note at the same time that for paraelectric centers the tunnel splitting depends as a rule on the temperature.[5] It is possible that as the temperature rises the tunneling proceeds more and more via excited vibronic states of the center, for which Δ is large, while for $T > 30$, owing to the rapid increase of the level width τ_2^{-1} the condition $\tau_2^{-1} > |\Gamma_{3,4}|$, at which phonon localization of the centers takes place,[2,11,20] begins to be met. Allowance for the excited states does not change the foregoing arguments and can be reduced to an effective change of the parameters of the theory.

The tunnel effects considered here can manifest themselves also in other resonance phenomena. Thus, in the presence of delocalization, paraelectric transitions can take place at frequencies close to $\nu \approx |\Gamma_i|$; the probabilities of these transitions are given by Eqs. (9) and (11) and are shown by the dashed lines of Fig. 2. These resonances can influence one another if paraelectric and EPR transitions are simultaneously excited. Such a double tunnel-magnetic resonance may be effective for the study of the tunnel splittings on centers with weak tunneling (when direct recording of the paraelectric resonances on them is difficult), by using the influence of the paraelectric resonances on the higher-frequency EPR transitions.

We note, finally, that all the foregoing conclusions remain in force if it is assumed, in accord with experiment, that the resonant magnetic fields are varied rather than the frequencies.

5. CONCLUSION

The previously investigated electric-field effects[6,8] differ from those considered here in that they pertain to centers localized in one of the structural positions, and no tunneling takes place in them. Most of these studies were made on objects having only one structural position. In the case of the so-called reorienting centers, which can have several positions, the electric-field effect was investigated, just as for one-structure centers, in only one of the positions (in which case the EPR could serve also as an indicator of their occupancy). A characteristic feature of all these studies is that they deal with effects connected with a change produced by the E-field in the parameters of the ordinary spin Hamiltonian that describes the resonant phenomena in the absence of an electric field (the so-called linear electric-field effect and its derivatives).

For tunnel electric-field effects to be observable the parameters that are specific to the effect, viz., the tunnel splitting Δ and the operator ME of the magnetic and electric fields between the states of the different minima of the adiabatic potential, must differ from zero. In addition to meeting this condition it is necessary to determine the relation between these parameters and the Zeeman and Stark energies in each of the wells. The conditions for realizing these effects in regions I and II are not equal and are connected with different parameters of the theory. Thus, in region I the parameter Δ by itself does not lead to any effects. It is also necessary here, howeer, to have the zeroth-approximation Stark and Zeeman energies almost equal. If the foregoing conditions are met, the frequencies and probabilities of the transitions turn out to be anomalously sensitive to the external electric field, and it is this which leads to the tunnel electric-field effects.

APPENDIX

Assume an arbitrary Hermitian quasi-diagonal matrix M such that $\overline{M}_{12} = \overline{M}_{34} = 0$. Interchanging rows and columns, it can be rewritten in the form of a new matrix m in which diagonal ME of simultaneously considered levels are located alongside one another. We generalize a method, proposed[17] for a group of degenerate levels, to include the case of arbitrary distance between a group of levels. To this end we carry out a unitary transformation $\overline{m} = v^{-1} m v$ that leads to $\overline{m}_{12} = \overline{m}_{34} = 0$. The quasi-diagonal matrix v and the ME $\overline{m}_{ij}$ differ from the matrix U and the ME $\overline{M}_{ij}$ by the substitution $M_{ij} \to m_{ij}$. Using as the zeroth approximation the diagonal ME $\overline{m}_{jj} = E_j^{(0)}$ and as the perturbation the off-diagonal ME, we obtain, accurate to second-order perturbation theory, the energies

$$E_j = E_j^{(0)} + \sum_{k \neq i,j} |\overline{m}_{jk}|^2 / (\overline{m}_{jj} - \overline{m}_{kk}) \tag{A.1}$$

and the coefficients of the wave functions

$$|g_{jj}| = 1, \quad g_{ij} = \frac{g_{jj}}{\overline{m}_{jj} - \overline{m}_{ii}} \sum_{k \neq i,j} \frac{\overline{m}_{ik} \overline{m}_{kj}}{\overline{m}_{jj} - \overline{m}_{kk}}, \quad g_{kj} = \frac{\overline{m}_{kj} g_{jj}}{\overline{m}_{jj} - \overline{m}_{kk}}. \tag{A.2}$$

The subscript i labels the level that enters together with the level j in one group, and the subscript k, levels of the other group. Equations (A.1) and (A.2), while formally in agreement with those given in Ref. 17, differ from the latter in having $m_{jj} \neq m_{ii}$.

For an arbitrary ME of the $i \to j$ transition due to a time-dependent perturbation, one can obtain

$$\gamma_{ij} = \sum_{\beta,\beta'}^{4} A_{\beta i}^* A_{\beta' j} M_{\beta\beta'}(t).$$

The matrix $M(t)$ coincides with the matrix M in which the field components must be regarded as dependent on the time, and $\Delta = 0$; A_{ij} are the expansion coefficients of the wave functions that serve as the basis of the matrix $\overline{m}$, in terms of the basis wave functions of the matrix M.

[1] B. I. Bersuker and V. Z. Polinger, Vibronic Interactions in Molecules and Crystals [in Russian], Nauka, 1983.
[2] V. I. Gol'danskiĭ, L. I. Trakhtenberg, and V. N. Flerov, Tunneling Phenomena in Chemical Physics [in Russian], Nauka, 1986.
[3] V. M. Svistunov, M. A. Belogolovskiĭ, and O. I. Chernyak, Usp. Fiz. Nauk **151**, 31 (1987) [Sov. Phys. Usp. **30**, 1 (1987)].
[4] I. B. Bersuker, Electronic Structure and Properties of Coordination Compounds [in Russian], Khimiya, 1986.
[5] U. Kh. Kopvillem and R. V. Saburova, Paraelectric Resonance [in Russian], Nauka, 1982.
[6] M. D. Glinchuk, V. G. Grachev, M. F. Deigen, *et al.*, Electric Effects in Microwave Spectroscopy [in Russian], Nauka, 1981.
[7] A. B. Roĭtsin, A. B. Brik, S. S. Ishchenko, *et al.*, Fiz. Tverd. Tela (Leningrad) **26**, 2968 (1984) [Sov. Phys. Sol. State **26**, 1792 (1984).
[8] V. B. Mims, Electro-field Effect in Paramagnetic Resonance [in Russian], Naukova dumka, 1982.
[9] A. B. Roĭtsin, Usp. Fiz. Nauk **105**, 677 (1971) [Sov. Phys. Usp. **14**, 766 (1971)].
[10] A. B. Brik and I. V. Matyash, Ukr. Fiz. Zh. **28**, 141 (1982).
[11] V. S. Vikhnin, Fiz. Tverd. Tela (Leningrad) **18**, 1468 (1976); **20**, 1340 (1978); **27**, 825 (1985) [Sov. Phys. Solid State **18**, 853 (1978); **20**, 771 (1978); **27**, 506 (1985).
[12] V. S. Vikhin, I. S. Sochava, and J. N. Tolparov, Defects in Insulating Crystals, Proc. Int. Conf., Riga. Springer, 1981, p. 601.
[13] A. B. Brik and V. S. Vikhnin, Fiz. Tverd. Tela (Leningrad) **28**, 1183 (1986) [Sov. Phys. Solid State **28**, 662 (1986)].

[14]I. B. Bersuker, V. G. Vekhter, and M. L. Rafalovich, Teor. Eksp. Khim. **8**, 737 (1972).
[15]A. B. Roĭtsin, Phys. Stat. Sol (b) 104, 11 (1981).
[16]A. B. Roĭtsin, Some Applications of Symmetry Theory in Microwave Spectroscopy Problems [in Russian], Naukova Dumka, 1973.
[17]L. D. Landau and E. M. Lifshitz, *Quantum Mechanics, Nonrelativistic Theory*, Pergamon.
[18]R. H. Nuttal and J. A. Weil, Can. J. Phys. **59**, 1709 (1981).
[19]A. B. Brik, I. V. Matyash, S. A. Litovchenko, and M. I. Samilovich, Fiz. Tverd. Tela (Leningrad) **22**, 3161 (1980) [Sov. Phys. Sol. State **22**, 1849 (1980)].
[20]M. I. Dykman and G. G. Tarasov, Zh. Eksp. Teor. Fiz. **73**, 1061 (1978) [Sov. Phys. JETP **46**, 562 (1978)].

Translated by J. G. Adashko